Local Structures in Crystalline and Amorphous Phases of Diglyme−$LiCF_3SO_3$ and Poly(ethylene oxide)−$LiCF_3SO_3$ Systems: Implications for the Mechanism of Ionic Transport

Christopher P. Rhodes and Roger Frech*

Department of Chemistry and Biochemistry, University of Oklahoma, Norman, Oklahoma 73019

Received October 10, 2000; Revised Manuscript Received January 31, 2001

ABSTRACT: The ability of ethylene oxide-based materials to dissolve salts and form ionically conducting systems has attracted widespread interest. Our molecular level understanding of ionic conductivity in these systems critically depends on our understanding of local structures. The crystal structure of diethylene glycol dimethyl ether:$LiCF_3SO_3$ or diglyme:$LiCF_3SO_3$ consists of diglyme−salt dimers with the lithium ion in a 5-fold coordination strikingly similar to that in crystalline poly(ethylene oxide)$_3$:$LiCF_3SO_3$. However, spectroscopic studies of diglyme−$LiCF_3SO_3$ solutions indicate that lithium ion is coordinated by only three oxygen atoms from a diglyme molecule and one oxygen atom from a $CF_3SO_3^-$ anion as part of a contact ion pair. A parallel spectroscopic study of high molecular weight PEO−$LiCF_3SO_3$ suggests that the ionically conducting amorphous phase also contains four-coordinate lithium ions in a local structure similar to that in the diglyme solution. Analysis of Raman and X-ray data of PEO−$LiCF_3SO_3$ films suggests that the amorphous phase contains local structures which resemble the structure present in crystalline P(EO)$_3$:$LiCF_3SO_3$. The significance of local structures for the mechanism of ion transport is discussed.

1. Introduction

Polymer electrolytes based on poly(ethylene oxide) with dissolved salts are of considerable interest for rechargeable lithium batteries and fundamental research of ionic transport in disordered phases. The mechanism of ionic transport in high molecular weight PEO−salt systems is poorly understood at the molecular level, although it is recognized that cation−anion interactions,[1] cation−polymer interactions,[2] and polymer segmental motion[3] play a critical role. The ionic conductivity of high molecular weight poly(ethylene oxide), PEO, with dissolved lithium trifluoromethanesulfonate, $LiCF_3SO_3$, has been found to occur primarily in an amorphous phase.[4,5] Determining the local structure of the ionically conducting phase serves to further our understanding of the microscopic mechanism of ionic conductivity within these systems. Vibrational spectroscopy has provided considerable information on the local structures in polymer electrolytes and is a particularly useful probe of local structure in the amorphous phase. To gain insight into the amorphous phase, two general strategies have been used: investigation of the crystalline phase(s) of the system[6−8] and use of low molecular weight analogues containing the ethylene oxide monomer as models.[9−11] Here both strategies are combined to advance our insight into the local structures present in the ionically conducting phase of PEO−$LiCF_3SO_3$. In turn this insight leads to a deeper understanding of the ionic transport mechanism in the system.

2. Experimental Section

Diethylene glycol dimethyl ether (diglyme), PEO ($M_v = 4 \times 10^6$), and $LiCF_3SO_3$ were obtained from Aldrich. Diglyme was used as received. $LiCF_3SO_3$ was heated under vacuum at 120 °C for 48 h, and PEO was dried under vacuum at 50 °C for 24 h. The reagents were stored and manipulated in a dry nitrogen glovebox (VAC, ≤1 ppm of H_2O). To prepare the diglyme:$LiCF_3SO_3$ crystals, a solution of $LiCF_3SO_3$ dissolved in diglyme at an ether oxygen:cation ratio of 5:1 was stirred for ∼48 h and left inside the glovebox at room temperature. An intermediate gellike phase appeared which then became crystalline after a number of months. Crystalline P(EO)$_3$:$LiCF_3SO_3$ was prepared by a method previously published.[12] The 10:1 diglyme−$LiCF_3SO_3$ solution was prepared by dissolving the salt directly in diglyme. To prepare the PEO−$LiCF_3SO_3$ films, stoichiometric amounts of PEO and $LiCF_3SO_3$ were combined with acetonitrile. For the pure PEO film, PEO was combined with acetonitrile. The solutions were stirred for 24 h, and then films were cast onto either Telfon (for Raman and differential scanning calorimetry (DSC) measurements) or glass slides (for X-ray diffraction measurements). The cast films were left in the glovebox for 24 h to evaporate solvent and then heated at 50 °C for 24 h under vacuum. The heating temperature was chosen to avoid heating the film above the melting point of PEO. The same sample preparation, heating temperature, and time were used for the Raman, X-ray, and DSC specimens to enable direct comparison of the data. Data on the films were taken within 1−2 h after removing the films from the vacuum oven.

A single-crystal specimen was isolated from the 5:1 diglyme−$LiCF_3SO_3$ solution for X-ray analysis. X-ray diffraction data were collected at 173(2) K on a Siemans P4 diffractometer using Mo Kα radiation (λ = 0.718 73 Å). The data were corrected for Lorentz and polarization effects; an absorption correction was not applied since it was judged to be insignificant. The structure was solved by the direct method using the SHELXTL system and refined by a full matrix least squares on F^2 using all reflections. All non-hydrogen atoms were refined anisotropically, and all hydrogen atoms were included in the refinement with idealized parameters. The final $R1 = 0.037$ is based on 3852 "observed reflections" ($I > 2\sigma(I)$), and the $wR2 = 0.099$ is based on all reflections (4566 unique data). For the PEO−$LiCF_3SO_3$ films, powder X-ray diffractograms were recorded at ambient conditions from $5 \leq 2\theta \leq 70$ in 2θ steps of 0.05° on a Rigaku D/4MAX automated diffractometer using Cu Kα radiation.

Raman scattering spectra were recorded on an I.S.A. Jobin-Yvon T64000 in the triple subtractive mode with a scan time

* Corresponding author.

10.1021/ma001749x CCC: $20.00
Published on Web 03/16/2001

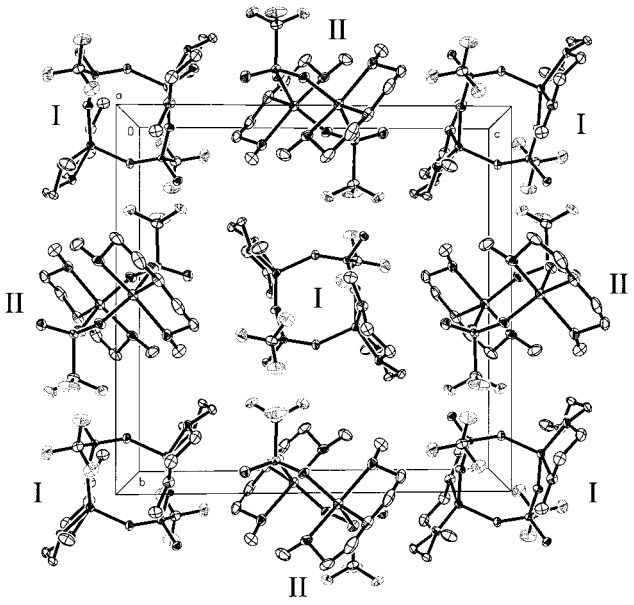

Figure 1. Packing diagram of crystalline diglyme:$LiCF_3SO_3$ showing type I and type II dimers. Hydrogen atoms are not shown in the diagram.

of 16 s and 10 accumulations using a 90° scattering geometry (for the diglyme−$LiCF_3SO_3$ system) and a 180° geometry (for the PEO−$LiCF_3SO_3$ system). The 514 nm line of an argon laser operating at 300 mW was used for excitation. Bands were curve-fit by the Levenberg−Marquardt method using Galactic Grams software. DSC thermograms were collected on a Mettler DSC 820 calorimeter under nitrogen purge in sealed aluminum crucibles. Data for the diglyme:$LiCF_3SO_3$ crystal were collected from 25 to −100 to 80 °C with a heating/cooling rate of 10 °C/min. Data for the PEO−$LiCF_3SO_3$ films and the $P(EO)_3$:$LiCF_3SO_3$ compound were collected from 25 to 220 °C with a heating rate of 10 °C/min. Ab initio calculations were performed using the B3LVP hybrid Hartree−Fock density functional method using the 6-31G(d) basis.

3. Results and Discussion

3.1. Diglyme−$LiCF_3SO_3$. We begin by reporting the discovery of the 1:1 compound of diglyme, $CH_3(OCH_2CH_2)_2OCH_3$, with $LiCF_3SO_3$, hereafter labeled diglyme:$LiCF_3SO_3$. A single crystal of the 1:1 compound was isolated, and its structure was determined by X-ray diffraction techniques. The compound provides an excellent opportunity to markedly extend our insight into local structures and their corresponding vibrational spectroscopic signatures in ethylene oxide-based systems containing dissolved salts. DSC measurements showed that the phase was stable to −100 °C and had an onset of melting at ∼27 °C. The compound crystallizes with $Z = 4$ in the monoclinic $P2_1/c$ space group with $a = 9.6117(10)$ Å, $b = 16.2782(13)$ Å, $c = 16.6202(15)$ Å, and $\beta = 93.549(8)°$. The asymmetric unit contains two independent halves of two dimers. Therefore, the unit cell consists of four dimers, two of which are identical and slightly different in structure from the other identical pair. An extended unit cell showing the two types of dimers is presented in Figure 1. Each dimer has a crystallographically imposed center of symmetry, with the inversion center lying at the midpoint between the two sulfur atoms of the triflate anions. Figure 2 shows the details of a single dimer. Every monomeric unit of the dimer contains a single lithium ion coordinated with the three oxygen atoms of a diglyme molecule. Two triflate anions then join the two diglyme molecules into a dimer through the coordination of two oxygen atoms of each triflate anion to the lithium ion associated with each diglyme molecule.

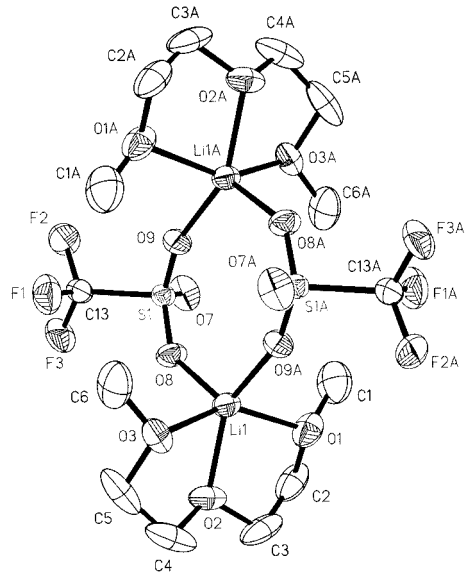

Figure 2. Crystal structure of diglyme:$LiCF_3SO_3$ showing the geometry of one dimer. Hydrogen atoms are not shown in the diagram.

Table 1. Lithium−Oxygen Bond Distances in Diglyme−$LiCF_3SO_3$ and $P(EO)_3$:$LiCF_3SO_3$ Crystals[a]

	diglyme:$LiCF_3SO_3$		
Li−O distance (Å)	dimer I	dimer II	$P(EO)_3$:$LiCF_3SO_3$
Li1−O1(ether oxy)	2.166	2.105	2.38(9)
Li1−O2(ether oxy)	2.044	2.075	1.72(7)
Li1−O3(ether oxy)	2.113	2.105	2.01(8)
Li1−O8 (trif oxy)	1.965	1.959	2.21(8)
Li1−O9A(trif oxy)	1.949	1.944	2.14(8)

[a] The data for the $P(EO)_3$:$LiCF_3SO_3$ compound were obtained from the published crystal structure parameters.[8] For the diglyme:$LiCF_3SO_3$ crystal, uncertainties are 0.003−0.004 Å for the bond distances. The specific distances and angles are defined based on the type I dimer (Figure 2), and the parameters for the type II dimer and $P(EO)_3$:$LiCF_3SO_3$ are for an analogous geometry as in the type I dimer.

Table 2. Oxygen−Lithium−Oxygen Bond Angles in Diglyme−$LiCF_3SO_3$ and $P(EO)_3$:$LiCF_3SO_3$ Crystals[a]

	diglyme:$LiCF_3SO_3$		
O−Li−O angle (deg)	dimer I	dimer II	$P(EO)_3LiCF_3SO_3$
O1−Li1−O2	77.0	78.0	85(3)
O2−Li1−O3	78.1	77.6	94(4)
O1−Li1−O3	146.2	141.9	174(5)
O8−Li1−O9A	108.8	109.1	112(4)
O2−Li1−O8	103.6	100.0	107(4)
O2−Li1−O9A	147.6	150.8	134(5)

[a] For the diglyme:$LiCF_3SO_3$ crystal, uncertainties are 0.2−0.4° for the bond angles. Further information on the parameters and labels are provided in the Table 1 footnote.

The crystal structure of the diglyme:$LiCF_3SO_3$ compound is remarkably similar to the crystal structure of the high molecular weight $P(EO)_3$:$LiCF_3SO_3$ compound. Selected lithium−oxygen bond lengths, oxygen−lithium−oxygen angles, and torsional angles in the two compounds are presented in Table 1, Table 2, and Table 3, respectively. From the comparison of distances and angles, it can be seen that the 5-fold coordination of the lithium ion in diglyme:$LiCF_3SO_3$ is remarkably similar to that observed in the crystal structure $P(EO)_3$:$LiCF_3$-

Table 3. Torsional Angles for the Ethylene Oxide Units in the Diglyme−$LiCF_3SO_3$ and $P(EO)_3$:$LiCF_3SO_3$ Crystals[a]

	diglyme:$LiCF_3SO_3$			
bond sequence	dimer I	dimer II	$P(EO)_3LiCF_3SO_3$	label
C1−O1−C2−C3	−177.4	159.0	−166.9	t
O1−C2−C3−O2	56.2	50.1	70.3	g
C2−C3−O2−C4	−175.9	−163.3	176.5	t
C3−O2−C4−C5	171.6	171.5	158.8	t
O2−C4−C5−O3	−55.3	−54.3	−44.1	g′
C4−C5−O3−C6	179.6	−175.5	−177.7	t
C−O−C−C			166.5	t
O−C−C−O			64.3	g
C−C−O−C			−162.4	t

[a] For the diglyme:$LiCF_3SO_3$ crystal, uncertainties are estimated to be 0.4−0.8° for the torsional angles. Further information on the parameters and labels is provided in the Table 1 footnote.

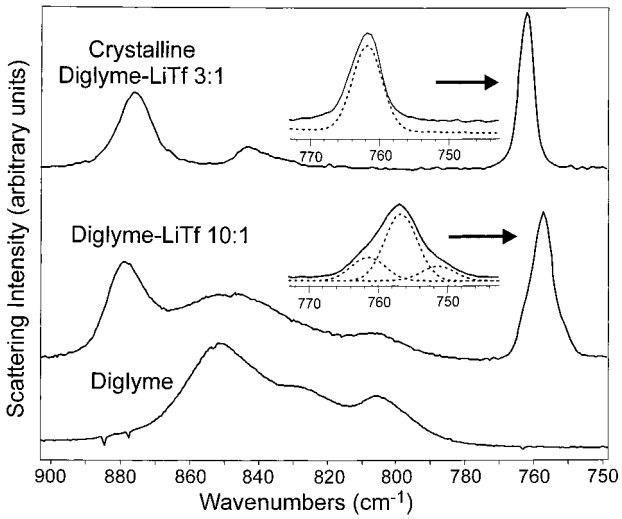

Figure 3. Raman spectra of crystalline diglyme:$LiCF_3SO_3$, diglyme−$LiCF_3SO_3$ solution with an ether oxygen:lithium ratio of 10:1, and pure diglyme in the region 700−900 cm^{-1}. The expanded views are curve-fitting analysis of the $\delta_s(CF_3)$ region.

SO_3. In both crystalline compounds, the lithium ion is coordinated by three oxygen atoms from the ethylene oxide chain and two oxygen atoms from different triflate anions. In the diglyme:$LiCF_3SO_3$ compound, the torsional angle sequence which coordinates the lithium ion is tgt-tg′t. In the $P(EO)_3$:$LiCF_3SO_3$ compound the torsional angle sequence is tgt-tg′t-tgt, and a closer inspection reveals that the unit coordinating the lithium contains three oxygen atoms and consists of the same torsional angle sequence tgt-tg′t with the additional tgt unit "linking" coordinating units.

Vibrational spectroscopy has proven to be a powerful technique to examine cation−anion interactions[13,14] and changes of the ethylene oxide backbone conformation[9,15] accompanying the interaction of the ether oxygen atoms with the cations. The spectroscopic data described here initially focuses on those intramolecular modes of the triflate ion whose frequencies are especially sensitive to interactions with the cations: the CF_3 symmetric deformation mode, $\delta_s(CF_3)$, and the SO_3 symmetric stretching vibration, $\nu_s(SO_3)$. The Raman spectrum of the crystalline diglyme:$LiCF_3SO_3$ compound in the $\delta_s(CF_3)$ region is shown in Figure 3. The single band at 763 cm^{-1} is due to the triflate ion $\delta_s(CF_3)$ mode. Similarly, a single $\nu_s(SO_3)$ band is observed in the crystal at 1053 cm^{-1} (data not shown). The observation of a single Raman-active triflate anion mode in these two spectral regions rather than the four modes predicted by a factor group vibrational analysis[12] can be explained by assuming that the triflate intramolecular vibrations are vibrationally coupled within each dimer but highly decoupled between the dimers in the unit cell. An isolated dimer with the formula $[CH_3O(CH_2CH_2O)_2CH_3LiCF_3SO_3]_2$ belongs to the C_i point group and accordingly yields a Raman-active mode of A_g symmetry and an infrared-active mode of A_u symmetry in both the $\delta_s(CF_3)$ region and the $\nu_s(SO_3)$ region. Although the two pairs of dimers in the unit cell have slightly different structures, the observation of just one band in each region demonstrates that the structural difference between the two kinds of dimers is not sufficient to allow a spectroscopic distinction between the two.

Table 4. Band Frequencies, Relative Percent Area, and Assignments of Triflate Anion Species from Curve-Fitting Analysis of Raman Spectra of the $\delta_s(CF_3)$ Region[a]

system	band (cm^{-1})	relative percent (%)	assignment
diglyme−LiTf (10:1)	762	23	aggregate
	757	63	ion pairs
	753	14	free ions
PEO−LiTf (10:1)	761	73	aggregate
	757	22	ion pairs
	753	5	free ions
PEO−LiTf (20:1)	761	29	aggregate
	757	65	ion pairs
	753	6	free ions

[a] Relative percent area is obtained by dividing the percent area for a specific band from the total area of all three bands. The error in percent area is estimated to be ±3%.

The $\delta_s(CF_3)$ and $\nu_s(SO_3)$ modes have been well-studied in a variety of ethylene oxide−lithium triflate systems. Both the $\delta_s(CF_3)$ band at 763 cm^{-1} and the $\nu_s(SO_3)$ mode at 1053 cm^{-1} have been assigned to the vibration of a triflate anion in which two of the three oxygen atoms of the anion are coordinated by lithium ions; i.e., the triflate anion essentially vibrates as a $[Li_2CF_3SO_3]^+$ entity.[16] As noted earlier, two oxygen atoms of a triflate ion are each coordinated with the lithium ion uniquely associated with a diglyme monomeric unit. Consequently, each triflate ion in the crystal vibrates as an $[Li_2CF_3SO_3]^+$ entity, and the observed frequencies of $\delta_s(CF_3)$ and $\nu_s(SO_3)$ can be easily understood in terms of the crystal structure.

It is revealing to compare the spectrum of the crystal in this region with the spectrum of a diglyme solution at a 10:1 (ether oxygen:cation) composition also shown in Figure 3. That spectrum consists of a broad asymmetric band which can be deconvolved into a major component at 757 cm^{-1}, assigned to contact ion pairs, and minor components at 753 and 761 cm^{-1}, attributed to "free" ions and $[Li_2CF_3SO_3]^+$ entities, respectively.[16] The curve-fitted bands are shown in Figure 3, and the contribution of each component band to the total integrated intensity is presented in Table 4. A comparison of the experimental splitting of the $\nu_{as}(SO_3)$ mode (not shown) with the calculated values[16] suggests that the Li···SO_3CF_3 ion pair is a monodentate structure rather than a bidentate structure. The major component of the $\nu_s(SO_3)$ band is observed at 1043 cm^{-1}, a frequency which has also been assigned to contact ion pairs.[17] It follows that the ionic species present in the 10:1 diglyme solution are predominantly ion pairs. The presence of a minor component at 762 cm^{-1} coincident (within error) with the frequency of the $\delta_s(CF_3)$ mode in the crystal suggests the presence of isolated dimers in the solution.

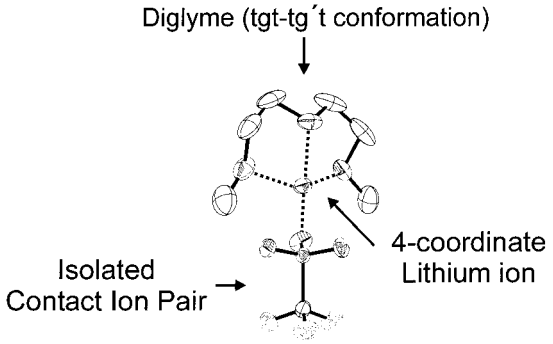

Figure 4. Pictoral representation of proposed local structure occurring in 10:1 solution of diglyme−$LiCF_3SO_3$ contianing a four-coordinate lithium ion, a diglyme molecule in a tgt-tg′t conformation, and an isolated triflate anion. Hydrogen atoms are not shown in the diagram.

The spectral region from 800 to 900 cm^{-1} (also shown in Figure 3) contains modes that are a mixture of CH_2 rocking and CO stretching motions.[18,19] These mode frequencies[19,20] and intensities[9] depend on the O−C−C−O torsional angle(s) and hence the backbone conformation. When a salt is dissolved in an ethylene oxide-based system, the interaction of the cation with the ether oxygen atoms changes the torsional angle(s).[9] The frequency shifts accompanying these interactions provide important insight into the change of local backbone structure occurring upon complexation with a cation. Computational and experimental studies suggest that the frequency of at least one band in this region increases with decreasing values of the O−C−C−O torsional angle.[20] In the spectrum of the diglyme:$LiCF_3SO_3$ crystal, the most intense band in this region is at 877 cm^{-1}, and an additional feature is present at 842 cm^{-1}. Since the structure of the crystal is known, these bands can be attributed to a mixture of CH_2 rocking and CO stretching vibrations resulting from the local structure of the diglyme molecule in diglyme:$LiCF_3SO_3$ which consists of the torsional angle sequence tgt-tg′t. The relatively high frequency of the 877 cm^{-1} band compared with the bands in pure diglyme (see Figure 3) reflects the smaller O−C−C−O torsional angles present in the crystal; torsional angles of 77.0° and −77.0° have been calculated by ab initio methods for the pure diglyme in a tgt-tg′t conformation.

The Raman spectrum of the 10:1 diglyme−$LiCF_3SO_3$ solution is presented in Figure 3. The observation of a band in the 10:1 solution at 877 cm^{-1}, the same frequency as in the crystal, is especially significant because it establishes that the diglyme molecule in solution is in a conformation with a O−C−C−O torsional angle sequence very similar to those in the diglyme:$LiCF_3SO_3$ crystal, almost certainly through the interaction of the lithium cation with all three oxygen atoms of the diglyme molecule. However, the dominant ionic species in the solution is a contact ion pair, as described earlier. Therefore, we conclude that the lithium ion is 4-fold coordinated in solution, interacting with three oxygen atoms from a diglyme molecule and one oxygen atom from a triflate anion as represented in Figure 4. The formation of the dimer units occurs in concentrated salt solutions and upon crystallization is accompanied by 5-fold coordination of the lithium ion. This analysis is supported by the correlation between the decrease in the relative amount of the ion pair species and the increase in the relative amount of the aggregate species as the salt concentration is increased.[21]

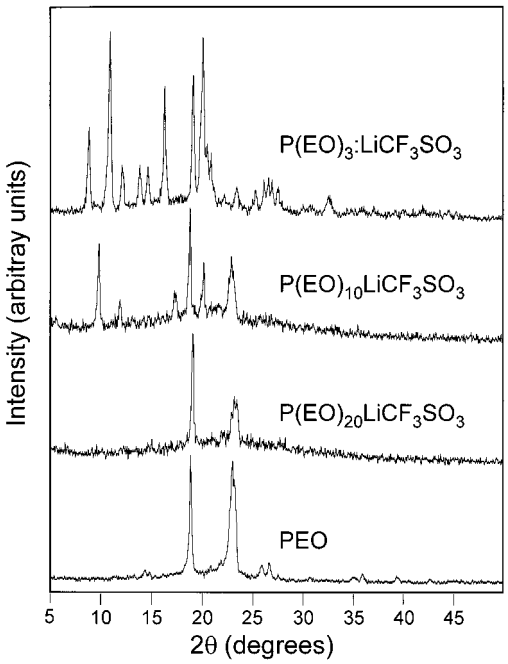

Figure 5. X-ray diffraction patterns for $P(EO)_3$:$LiCF_3SO_3$, $P(EO)_{10}LiCF_3SO_3$, $P(EO)_{20}LiCF_3SO_3$, and pure PEO.

3.2. Poly(ethylene oxide)−$LiCF_3SO_3$. The phase diagram of PEO−$LiCF_3SO_3$ has been previously reported.[7,22] At room temperature for salt concentrations up to 3:1, two phases are reported to be present, crystalline PEO and crystalline polymer−salt compound $P(EO)_3$:$LiCF_3SO_3$. Subsequent studies of the system have shown that in addition to these two phases an amorphous phase is present, and this amorphous phase is primarily where the ionic conductivity occurs.[4,5] Differences in the structures and properties of the PEO−$LiCF_3SO_3$ system have been observed and are attributed to differences in the molecular weight of the polymer,[23] the sample preparation method,[24] the thermal history,[25] and time.[26] Studies of pure PEO demonstrate the importance of molecular weight on the morphology and the degree of crystallinity.[27,28] For PEO−salt systems with different molecular weights of PEO, different relative amounts of ionic species were observed,[23] and the relative amounts of ionic species are dependent on temperature and time.[26] For samples with same salt concentration, various thermal histories were found to give different ionic conductivities.[25] These observed differences highlight the overall importance of kinetics, particularly crystallization kinetics, for both crystalline PEO and crystalline $P(EO)_3$:$LiCF_3SO_3$, in determining the state of the system.

To examine the local structure of the room-temperature amorphous phase of high molecular weight PEO−$LiCF_3SO_3$, films with a 10:1 and 20:1 composition were compared to crystalline $P(EO)_3$:$LiCF_3SO_3$ and crystalline PEO. The X-ray data are presented in Figure 5. We note that the X-ray data for this study are different than reported in a previous study,[7] and we attribute the difference to the different molecular weight of PEO used and different heating temperature and time used. The comparison of the 10:1 and 20:1 samples to pure PEO shows that both samples contain domains of crystalline PEO. Comparison of the 20:1 sample to crystalline $P(EO)_3$:$LiCF_3SO_3$ shows that the sample contains no

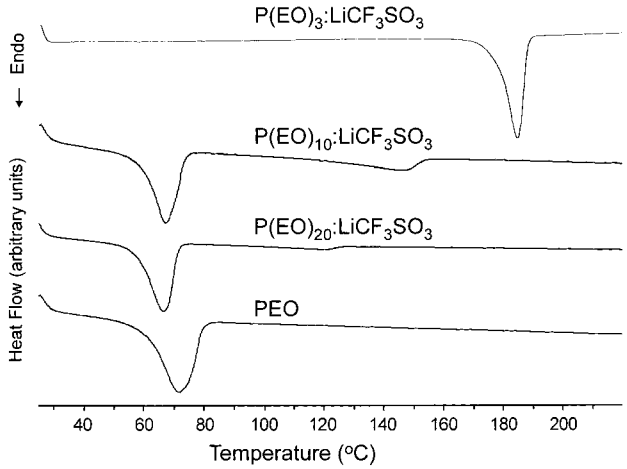

Figure 6. DSC thermograms of the crystalline $P(EO)_3$:$LiCF_3SO_3$ compound and films of $P(EO)_{10}LiCF_3SO_3$, $P(EO)_{20}LiCF_3SO_3$, and pure PEO.

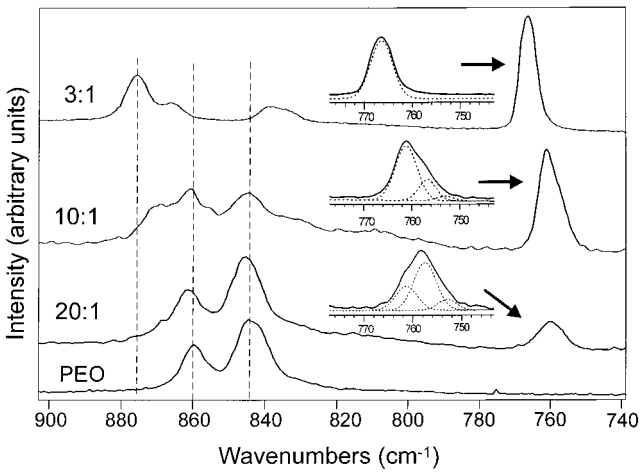

Figure 7. Raman spectra of crystalline $P(EO)_3$:$LiCF_3SO_3$, PEO−$LiCF_3SO_3$ complex with an ether oxygen:lithium ratio of 10:1, and pure PEO in the region 700−900 cm^{-1}. The expanded views are curve-fitting analysis of the $\delta_s(CF_3)$ region.

diffraction peaks that can be identified with the 3:1 crystalline compound. It is possible that this sample contains domains of crystalline $P(EO)_3$:$LiCF_3SO_3$ whose sizes are sufficiently small so that distinct peaks are not observed. In the 10:1 sample a few diffraction peaks are observed which coincide with peaks of the 3:1 compound. However, there are at least two peaks that are not present in the 3:1 crystal, suggesting that there is ordering present in the 10:1 sample that is different than the ordering present in the crystal. This ordering may be due to regions or domains with a structure similar to but not identical with structure in the crystalline $P(EO)_3$:$LiCF_3SO_3$. Possible structures will be discussed further below. As in the case for the 20:1 sample, the 10:1 sample may also contain domains of crystalline $P(EO)_3$:$LiCF_3SO_3$ whose sizes are sufficiently small so that distinct peaks are not observed.

DSC thermograms of the 10:1 and 20:1 samples are compared to thermograms of pure PEO and $P(EO)_3$:$LiCF_3SO_3$ in Figure 6. Both the 10:1 and 20:1 films clearly show the presence of an endotherm peak at 66 °C corresponding to the melting of crystalline PEO. The higher temperature of the melting endotherm in pure PEO compared to the melting endotherm in the PEO−LiTf films may be explained by the large crystallite sizes in pure PEO and the relatively fast heating rate. The 10:1 sample has a weak endotherm peak at 145 °C, and the 20:1 sample has a very weak endotherm peak at 120 °C. According to the phase diagram, these peaks indicate the presence of very small amounts of the crystalline $P(EO)_3$:$LiCF_3SO_3$ compound. A comparison of the data for the 10:1 and 20:1 films to previous DSC studies of the system[4,5,29] shows that the specific sample preparation used for this study, most notably heating below the melting point of PEO, produces very small amounts of the $P(EO)_3$:$LiCF_3SO_3$ phase.

Raman spectra of the 10:1 and 20:1 samples are shown in Figure 7. The $\delta_s(CF_3)$ region can be deconvolved into a minor "free" ion component at 753 cm^{-1}, a contribution from contact ion pairs at 757 cm^{-1}, and a dominant band at 761 cm^{-1} originating in the $[Li_2CF_3SO_3]^+$ entity. The relative percent of these species is summarized in Table 4. The 10:1 sample has more of the $[Li_2CF_3SO_3]^+$ aggregate and less of the ion pair species compared to the 20:1 sample. We again note that the relative amounts of the three components may depend on the sample preparation, thermal history, and aging. The crystalline $P(EO)_3$:$LiCF_3SO_3$ compound has only a single band at 766 cm^{-1},[12] also shown in Figure 7. The frequency of this band, 766 cm^{-1}, is higher than the frequency observed for the $[Li_2CF_3SO_3]^+$ aggregate in the diglyme:$LiCF_3SO_3$ crystal and for similar species in solution, 763 cm^{-1},[16] and we attribute the higher frequency to crystal packing effects present in the $P(EO)_3$:$LiCF_3SO_3$ compound. Support for the well-ordered potential energy environment of the triflate anion in the $P(EO)_3$:$LiCF_3SO_3$ crystal is the frequency difference between the Raman and infrared bands which indicates a modest amount of dynamical coupling.[12] The observed frequency of the $[Li_2CF_3SO_3]^+$ species, 761 cm^{-1}, in both the 10:1 and 20:1 sample argues that the local potential energy environment of the triflate anion is different than that present in the crystal. This analysis is supported by the X-ray data for the 10:1 sample which shows different *d* spacings than are present in the crystal.

Also shown in Figure 7 are the mixed CH_2 rocking and CO stretching modes. Bands in the 10:1 sample at 861 and 845 cm^{-1} (second and third dashed lines) are easily identified as contributions from the crystalline PEO fraction, whose spectrum in this region is also shown. Of particular interest in the 10:1 sample is the band at 870 cm^{-1} and a broad feature at approximately 830 cm^{-1}; these features can be identified with bands at 875 (first dashed line) and 836 cm^{-1} in the 3:1 crystalline compound. Therefore, the local conformational structure of the polymer backbone in the 10:1 material is similar to, but not identical with, the analogous structure in the crystalline compound. This difference again reflects, in part, the disordered nature of the system. The broad band between 800 and 820 cm^{-1}, which appears in the Raman spectra of PEO above its melting point,[30] shows that the amorphous phase contains a distribution of backbone conformational sequences similar to PEO in the melt. The spectra of the 20:1 sample in this region show bands at 861 and 845 cm^{-1} due to PEO and show a slight shoulder on the high-frequency side of the 860 cm^{-1} band. The 20:1 sample has no observable bands which can be clearly identified with the $P(EO)_3$:$LiCF_3SO_3$ compound.

We consider the nature of the local structures present in the 10:1 and 20:1 samples. Within the PEO−$LiCF_3SO_3$ films there exists crystalline PEO, small domains

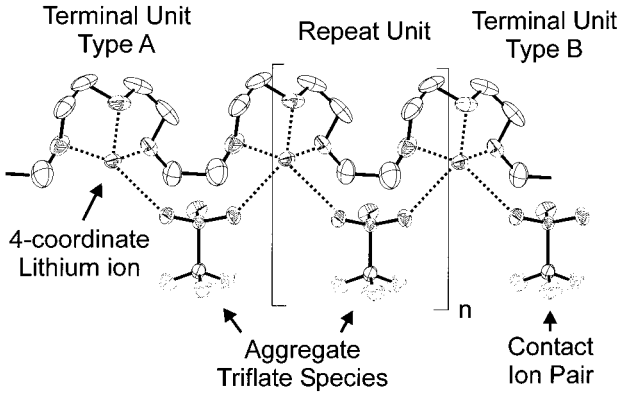

Figure 8. Pictorial representation of proposed localized complex occurring in 10:1 PEO−$LiCF_3SO_3$. For ease of graphic representation, the adjoining segments of the PEO chain are represented in an unfavored conformation. A more accurate pictorial representation would have the PEO chain in a tgt-tg′t-tgt conformation with the CF_3 end of the triflate anions on opposite sides of the chain. Hydrogen atoms are not shown in the diagram.

of crystalline $P(EO)_3$:$LiCF_3SO_3$, and a disordered phase. We earlier noted the two additional peaks seen in the X-ray data of the 10:1 sample and suggested that these result from a small amount of ordering present in the (primarily) disordered phase. It is not impossible that these reflections originate in a second ordered phase, although no such phase has ever been reported, especially at this salt concentration. Comparison of the 10:1 and 20:1 PEO−$LiCF_3SO_3$ films to the crystalline $P(EO)_3$:$LiCF_3SO_3$ compound shows that clear differences are present: the X-ray data show different diffraction peaks, the frequency of the $[Li_2CF_3SO_3]^+$ aggregate is different, and the frequencies of CH_2 rocking and CO stretching bands do not directly coincide with those present in the crystal. However, the frequency of aggregate species observed in the $\delta_s(CF_3)$ mode and the 10:1 X-ray data suggest that a local structure is present which is similar to the local structure present in the crystalline $P(EO)_3$:$LiCF_3SO_3$ phase. Therefore, we propose that within the disordered phase there exist numerous small regions (we will refer to such a region as a localized complex) where a few lithium ions and triflate ions form local structures with the polymer backbone that resemble the crystalline $P(EO)_3$:$LiCF_3SO_3$ phase. This perspective is supported by comparison of ^{13}C chemical shifts in amorphous PEO and crystalline $P(EO)_3$:$LiCF_3SO_3$ which suggest that a similar coordination of lithium to the ether oxygens is present in the amorphous phase as is present in $P(EO)_3$:$LiCF_3SO_3$.[31] Details of the proposed local structure are described below. Specifically, each lithium ion is 3-fold coordinated by adjacent polymer oxygen atoms. Further, as in the crystal, triflate ions link adjacent lithium ions, leading to 5-fold coordinate lithium ions and triflate ions vibrating as $[Li_2CF_3SO_3]^+$ entities. A representation of a localized complex is presented in Figure 8. The complex consists of n repetitions of a repeat unit bounded with terminal groups on each end. The repeat unit is essentially the local structure found in crystalline $P(EO)_3$:$LiCF_3SO_3$. The localized complex may be quite small ($n = 0$) or may be an extended structure (n = large). The terminal unit of the localized complex contains either a four-coordinate lithium ion and a terminal $[Li_2CF_3SO_3]^+$ entity (type A) or a five-coordinate lithium ion and a terminal Li−CF_3SO_3 contact ion pair (type B). As a sidenote, we envision a critical, early step in the growth of the crystalline $P(EO)_3$:$LiCF_3SO_3$ compound to occur through the extension and coalescence of these localized regions to form long chain lengths of the line compound. The formation of microcrystalline domains then results when several of these extended regions are brought into translational registry through attractive interchain forces, although the domain size may be so small as to yield only weak, extremely broad features in an X-ray diffraction measurement.

We also assume the existence of isolated species such as $[Li_2CF_3SO_3]^+$ units, Li−CF_3SO_3 contact ion pairs, and solvent-separated ion pairs (spectroscopically "free" ions) along the chain. We propose a local structure of the isolated contact ion pair to be analogous to the structure proposed for the diglyme−LiTf solution (Figure 4) with the ethylene oxide repeat units replacing the terminal methyl groups present in diglyme.

3.3. Implications for Ionic Transport in High MW PEO−$LiCF_3SO_3$. We consider the role of these local structures in ionic transport. The terminal unit of a localized complex, an isolated $[Li_2CF_3SO_3]^+$ species, and an isolated contact ion pair each contains 4-fold coordinate lithium ions. A "free" lithium ion may have an even lower effective coordination number. These lithium ions are coordinated by a potential energy environment that is dynamically disordered through polymer segmental motion and presumably less deep than 5-fold coordinated lithium in crystalline domains of $P(EO)_3$:$LiCF_3SO_3$. In the spirit of the dynamic bond percolation (DBP) model,[3,32] it follows that polymer segmental motion is more likely to open transient conduction pathways for lithium ions with relative low coordination numbers. Therefore, we argue that 4-fold coordinate lithium ions as part of a terminal unit of a localized complex, an isolated $[Li_2CF_3SO_3]^+$ species, and a contact ion pair species contribute to the ionic conductivity in the amorphous phase. We wish to emphasize that it is not the contact ion pair itself that contributes to the conductivity, because the diffusion of a neutral, discrete contact ion species would not contribute to the ionic conductivity as is well-known. Instead, the contribution comes from the lithium ion (and triflate ion) resulting from a dissociative process that underscores the dynamical nature of the equilibrium between the various ionic species present. We note that the time scale of the dissociative process of contact ion pairs, whether isolated or part of a localized complex, is a critical factor in their contribution to the ionic conductivity.

The involvement of the anion in ionic transport in these systems is supported by transference number measurements[33−35] and recent neutron scattering experiments.[36] From spectroscopic studies it is known that the anion exists as a "free" ion, a Li−CF_3SO_3 contact ion pair, and a $[Li_2CF_3SO_3]^+$ entity on a time scale of at least several vibrational periods (femtoseconds). It is also important to recognize the important role played by the terminal units of a localized complex in the transport of anions. Consider a localized complex with a terminal Li−CF_3SO_3 contact ion pair such as a type B structure shown in Figure 4. The potential energy environment of the triflate anion is defined primarily by the interaction with the cation of the contact ion pair; there is only a very weak interaction with the polymer itself. This is a marked contrast to the much stronger interaction of the cation with its coordinative environment of oxygen atoms. As a consequence, we expect the

transport mechanism of the triflate ion to be significantly different than that of the cation. A similar conclusion follows from considering an isolated contact ion pair. In both instances the arguments presented here would result in a highly labile anion. This perspective supported by measurements of the cation and anion diffusion coefficients in PEO−$LiCF_3SO_3$ which show that the anion is more mobile than the cation.[37,38] The actual contribution to the ionic conductivity might be mediated by other factors such as the steric interaction of the anion with the host matrix.

4. Conclusions

We have isolated and characterized a crystalline phase of diglyme−$LiCF_3SO_3$. In the diglyme:$LiCF_3SO_3$ crystal, the local environment of the Li ion and the torsional angle sequence of the bonds in the ethylene oxide units are remarkably similar to those present in the high molecular weight $P(EO)_3$:$LiCF_3SO_3$ compound. A comparison of the Raman bands in a 10:1 diglyme−$LiCF_3SO_3$ solution to the Raman bands in the diglyme:$LiCF_3SO_3$ crystal suggests that in the solution Li may be four-coordinate.

Raman, X-ray data, and DSC data of PEO−$LiCF_3SO_3$ films prepared at several compositions show that local structures are present which are similar but not identical with local structures present in the $P(EO)_3$:$LiCF_3SO_3$ crystal. Further work to determine the specific ordering which is observed in the 10:1 sample is currently in progress. We propose that in the "amorphous" phase of the polymer−salt system there exist microscopic domains of salt-rich regions whose local structures may resemble the crystalline compound phase. These microscopic domains may be localized regions of a single polymer chain as described above or even several adjacent localized regions in translational registry. In any case the cations and anions at the boundaries of these salt-rich regions are relatively mobile because of two factors: their potential energy environments are less attractive than in the interior of the microscopic domains, and those environments are dynamically disordered through the increased motion of the polymer chains in the interface. Therefore, we suggest that the ions at the domain boundaries make a significant contribution to the ionic conductivity, although we emphasize that this model does not necessarily describe the sole mechanism of ionic transport in polymer salt systems. Finally, we note that although this model has been developed for the PEO−$LiCF_3SO_3$ system, its general features can be extended to describe ionic transport in other polymer−salt electrolytes.

Acknowledgment. We acknowledge Masood Kahn for his assistance with the single X-ray diffraction analysis. This work was partially supported by funds from the Oklahoma Center for the Advancement of Science and Technology, Contract No. 5377. We appreciate the assistance of Scott Boesch in the ab initio calculations.

Supporting Information Available: Single X-ray diffraction data file (.cif file) containing fractional coordinates and additional structural information. This material is available free of charge via the Internet at http://pubs.acs.org.

References and Notes

(1) Papke, B. L.; Ratner, M. A.; Shriver, D. F. *J. Electrochem. Soc.* **1982**, *129*, 1434−1438.
(2) Armand, M. B.; Chabagno, J. M.; Duclot, M. J. Polyethers as solid electrolytes. In *Fast Ion Transport in Solids*; Vashista, P., Mundy, J. M., Shenoy, G. K., Eds.; Elsevier: Amsterdam, 1979; pp 131−136.
(3) Ratner, M. A.; Nitzan, A. *Faraday Discuss. Chem. Soc.* **1989**, *88*, 19−42.
(4) Berthier, C.; Gorecki, W.; Minier, M. *Solid State Ionics* **1983**, *11*, 91−95.
(5) Minier, M.; Berthier, C.; Gorecki, W. *J. Phys. (Paris)* **1984**, *45*, 739−744.
(6) Stainer, M.; Hardy, L. C.; Whitmore, D. H.; Shriver, D. F. *J. Electrochem. Soc.* **1984**, *131*, 784−790.
(7) Robitaille, C. D.; Fauteux, D. *J. Electrochem. Soc.* **1986**, *133*, 315−325.
(8) Lightfoot, P.; Mehta, M. A.; Bruce, P. G. *Science* **1993**, *262*, 883−885.
(9) Frech, R.; Huang, W. *Macromolecules* **1995**, *28*, 1246−1251.
(10) Sutjianto, A.; Curtiss, L. A. *J. Phys. Chem. A* **1998**, *102*, 968−974.
(11) Johansson, P.; Tegenfedlt, J.; Lindgren, J. *J. Phys. Chem. A* **1998**, *102*, 4660−4665.
(12) Rhodes, C. P.; Frech, R. *Solid State Ionics* **2000**, *136−137*, 1131−1137.
(13) Papke, B. L.; Ratner, M. A.; Shriver, D. F. *J. Phys. Chem. Solids* **1981**, *42*, 493−500.
(14) Schantz, S.; Sandahl, J.; Borjesson, L.; Torell, L. M.; Stevens, J. R. *Solid State Ionics* **1988**, *28−30*, 1047−1053.
(15) Frech, R.; Huang, W. *Solid State Ionics* **1994**, *72*, 103−107.
(16) Huang, W.; Frech, R.; Wheeler, R. A. *J. Phys. Chem.* **1994**, *98*, 100−110.
(17) Peterson, G.; Jacobsson, P.; Torell, L. M. *Electrochim. Acta* **1992**, *37*, 1495−1497.
(18) Yoshida, H.; Matsuura, H. *J. Phys. Chem. A* **1998**, *102*, 2691−2699.
(19) Matsuura, H.; Fukuhara, K. *J. Polym. Sci., Part B* **1986**, *24*, 1383−1400.
(20) Murcko, M. A.; DiPaola, R. A. *J. Am. Chem. Soc.* **1992**, *114*, 10010−10018.
(21) Petrowsky, M.; Rhodes, C. P.; Frech, R. *J. Solution Chem.*, submitted.
(22) Vallée, A.; Besner, S.; Prud'homme, J. *Electrochim. Acta* **1992**, *37*, 1579−1583.
(23) Brodin, A.; Mattsson, B.; Nilsson, K.; Torell, L. M.; Hamara, J. *Solid State Ionics* **1996**, *85*, 111−120.
(24) Weston, J. E.; Steele, B. C. H. *Solid State Ionics* **1982**, *7*, 81−88.
(25) Yang, L.; Zhang, A.; Qiu, B.; Yin, J.; Liu, Q. *Solid State Ionics* **1988**, *28−30*, 1029−1031.
(26) Chintapalli, S.; Frech, R. *Electrochim. Acta* **1998**, *43*, 1395−1400.
(27) Godovsky, Y. K.; Slonimsky, G. L.; Garbar, N. M. *J. Polym. Sci., Part C* **1972**, *38*, 1−21.
(28) Maclaine, J. Q. G.; Booth, C. *Polymer* **1975**, *16*, 680−684.
(29) Frech, R.; Chintapalli, S.; Bruce, P. G.; Vincent, C. A. *Macromolecules* **1999**, *32*, 808−813.
(30) Maxfield, J.; Shepherd, I. W. *Polymer* **1975**, *16*, 505−509.
(31) Spevacek, J.; Dybal, J. *Macromol. Rapid Commun.* **1999**, *20*, 435−439.
(32) Druger, S. D.; Ratner, M. A.; Nitzan, A. *Solid State Ionics* **1983**, *9* & *10*, 1115−1120.
(33) Bouridah, A.; Dalard, F.; Deroo, D.; Armand, M. B. *J. Appl. Electrochem.* **1987**, *17*, 625−634.
(34) Munshi, M. Z. A.; Owens, B. B.; Nguyen, S. *Polym. J.* **1988**, *20*, 597−602.
(35) Walls, H. J.; Zawodzinski, T. A. J. *Electrochem. Solid-State Lett.* **2000**, *3*, 321−324.
(36) Mao, G.; Perea, R. F.; Howells, W. S.; Price, D. L.; Saboungi, M.-L. *Nature* **2000**, *405*, 163−165.
(37) Bhattacharja, S.; Smoot, S. W.; Whitmore, D. H. *Solid State Ionics* **1986**, *18* & *19*, 306−314.
(38) Boden, N.; Leng, S. A.; Ward, I. M. *Solid State Ionics* **1991**, *45*, 261−270.

MA001749X